

Effects of Counterion on Protein Adsorption in Macroporous and Polymer-Grafted Cation Exchangers

Bachelorthesis 2

In Partial Fulfillment of the Requirements for the
Degree

“Bachelor of Science in Engineering“

Study program:

“Environmental engineering- and Biotechnology“

Management Center Innsbruck

Advisor:

Dr. Giorgio Carta (external)

Dr. Christoph Griesbeck (internal)

Author:

Bianca Glatz

0810351050

Declaration in lieu of oath

I hereby declare, under oath, that this bachelor thesis has been my independent work and has not been aided with any prohibited means. I declare, to the best of my knowledge and belief, that all passages taken from published and unpublished sources or documents have been reproduced whether as original, slightly changed or in thought, have been mentioned as such at the corresponding places of the thesis, by citation, where the extent of the original quotes is indicated.

The paper has not been submitted for evaluation to another examination authority or has been published in this form or another.

Innsbruck, am 02. September 2011

Acknowledgements

I would like to thank those people who aided me in the past months in order to complete this thesis, especially:

Dr. Giorgio Carta, my advisor at the University of Virginia, for giving me the opportunity to work in his group and for his great guidance, support and patience.

Ernie - for his advice in any kind of issue - no matter how busy he was.

Tarl, Rachel and Yige, for their warm welcome, their help and all the funny moments we shared.

The faculty members of my study program at the Management Center Innsbruck for the organizational support.

The Austrian Marshall Plan Foundation for the financial support.

Finally, I would like to thank the most inspiring people in my life: my parents, for their endless love, encouragement and being my role models.

Abstract

Separation and purification of proteins is playing a major role in Biopharmaceutical Drug Development. Therefore, chromatography provides a suitable unit operation for processing proteins in order to manufacture the desirable therapeutic agent. Ion exchange chromatography is most widely used and accounts for many of the steps included in protein purification protocols in industrial production. To optimize process performance of the stationary phase, an in-depth understanding of the adsorption behavior is required.

For this purpose the focus of this work is to investigate the effect of counterion on protein adsorption in two different types of cation exchangers. UNOsphere S, which consists of rigid macroporous polymer based particles, and Capto S, which is a crosslinked agarose matrix with charged dextran polymer grafts.

It is well known that the diffusion of counterion generally is coupled according to the Nernst-Planck equations. However, it is unknown to what extent this is a factor in protein adsorption. In this regard two different hypotheses are advanced. The first hypothesis postulates that protein transport in Capto S is enhanced by electrostatic coupling of the diffusion fluxes between the fast diffusing counterions and the slow diffusing protein. In this connection, electrostatic coupling is described by the Nernst-Planck equations. The second hypothesis postulates that protein transport is enhanced by a solid diffusion mechanism driven by a large adsorbed concentration driving force and by mobility in the adsorbed phase. In order to validate these hypotheses, equilibrium binding capacities of the two different stationary phases and the effective diffusivity, binding strength and binding charge of the model protein were determined. Based on their molecular properties, four different counterions were chosen: sodium, calcium, arginine and tetrabutylammonium hydroxide.

It was shown that calcium is held more tightly by both resins making the protein-calcium-exchange less favorable than the protein-sodium-exchange. In UNOsphere S the counterion has no effect in regard to the mass transfer kinetics, which was expected due to the fact that pore diffusion is predominant. Only a relatively small effect was seen in Capto S, suggesting that none of the two proposed hypotheses is appropriate for describing diffusion of the model protein in Capto S, which could be explained by the possibility that protein binding capacity rather than protein binding strength is more directly responsible for protein transport in Capto S.

Table of Contents

List of Symbols and Abbreviations.....	VI
List of Figures.....	VIII
List of Tables.....	IX
1. Introduction	1
2. Background.....	2
2.1. Chromatography in general.....	2
2.1.1. Chromatography in biopharmaceutical operations.....	2
2.2. Cation exchange chromatography (CEX).....	3
2.2.1. Different types of cation exchange matrices.....	4
2.3. Mass transfer effects.....	5
2.3.1. Pore diffusion.....	6
2.3.2. Solid diffusion.....	8
2.4. Counter diffusion (Nernst-Planck effect).....	10
3. Goals and objectives.....	11
4. Experimental techniques.....	13
4.1. Materials.....	13
4.1.1. Particlesizedistributions.....	13
4.1.2. Properties of the stationary phase.....	14
4.1.3. Lysozyme as model protein.....	15
4.1.4. Counterion properties.....	17
4.2. Adsorption isotherms.....	18
4.2.1. The Langmuir Model.....	19
4.2.2. The steric mass action model.....	19
4.3. Linear gradient elution.....	21
4.4. Batch uptakes kinetics.....	24
5. Results and discussion.....	26
5.1. Adsorption isotherms.....	26
5.2. LGE.....	29
5.3. Batch uptakes.....	35
5.4. Summarized conclusions and outlook.....	38
6. References.....	XI

List of Symbols and Abbreviations

c	protein concentration in the particle pores (mg/ml or mM)
C	fluid phase protein concentration (mg/ml or mM)
C_0	initial fluid phase protein concentration (mg/ml)
C_i	counterion concentration (mM)
C_M^R	counterion concentration at which peak elutes (mM)
CV	column volume
d_p	particle diameter (cm)
\bar{d}_p	mean particle diameter (μm)
D_e	effective pore diffusivity in pore diffusion model (cm^2/s)
D_s	adsorbed phase diffusivity in solid diffusion model (cm^2/s)
D_0	free solution diffusivity (cm^2/s)
k'	chromatographic retention factor
K	equilibrium constant in Langmuir isotherm model (ml/mg)
K_e	equilibrium constant for protein-counterion exchange
kDa	kilo Dalton
L	column length (cm)
q	adsorbed protein concentration (mg/ml)
\bar{q}	particle-average adsorbed protein concentration (mg/ml)
q^*	adsorbed protein concentration in equilibrium with external solution (mg/ml or mM)
q_m	single component maximum protein binding capacity (mg/ml)
r	particle radial coordinate (cm)
r_m	solute hydrodynamic radius (nm)
r_{pore}	pore radius (nm)
r_p	particle radius (cm)
t	time (s)

t_G	gradient duration (s)
TBAH	tetra butyl ammoniumhydroxide
u	linear flow velocity (cm/s)
v	interstitial mobile phase velocity (cm/s)
v'	reduced velocity
V	solution volume (ml)
V_M	volume of particles (ml)
z	protein effective binding charge

Greek Symbols

β	gradient slope, mM/min
γ	normalized gradient slope (mM)
δ	stagnant film thickness
ε	extraparticle porosity
ε_p	total intraparticle porosity
ε_{pM}	particle macroporosity
σ	hindrance factor in SMA model
ψ_p	diffusional hindrance factor
τ_p	tortuosity factor

List of Figures

Figure 1: General pore structure of rigid porous materials [2]	4
Figure 2: General pore structure of composite materials [2]	4
Figure 3: External mass transfer models [2]	6
Figure 4: Schematic drawing of pore diffusion mechanism	7
Figure 5: Schematic drawing of solid diffusion	8
Figure 6: Particle size distribution for (a) UNOsphere S and (b) Capto [4]	13
Figure 7: Lysozyme - Net charge vs. pH [2]	15
Figure 8: Lysozyme - molecular structure [3]	16
Figure 9: Drawing of the steric mass action model [2]	20
Figure 10: LGE relationship for ion exchange chromatography [2]	22
Figure 11: Flow scheme of the batch uptake apparatus [4]	24
Figure 12: Adsorption isotherms on UNOsphere S	26
Figure 13: Adsorption isotherms on Capto S	28
Figure 14: LGE chromatographic peaks for sodium	29
Figure 15: LGE chromatographic peaks for calcium	30
Figure 16: LGE chromatographic peaks for arginine	31
Figure 17: LGE summary normalized gradient slope vs. counterion concentration	32
Figure 18: LGE summary retention factor vs. counterion concentration	32
Figure 19: LGE chromatographic peaks for TBAH	34
Figure 20: Batch uptake curves on UNOsphere S	35
Figure 21: Batch uptake curves on Capto S	36

List of Tables

Table 1: Summary of stationary phase properties [4].....	14
Table 2: Species of counterions and their respective diffusivity values	17
Table 3: Summary of maximum lysozyme binding capacities for UNOsphere S	27
Table 4: Summary of isotherm results on Capto S.....	28
Table 5: LGE summary retention factor as a function of the counterion concentration.	33
Table 6: LGE summary protein charge & equilibrium parameter.....	33
Table 7: Summary of batch uptake results for UNOsphere S	36
Table 8: Summary of batch uptake results for Capto S.....	37

1. Introduction

As the biotechnological industry has grown rapidly over the past several years, the demand for larger scale and more efficient processes for the separation, purification and concentration of biomolecules, is increasing. Although many different types of processes are possible, adsorptive techniques like chromatography play a major role in these applications.

Due to its mild processing conditions and high resolving power chromatography is used extensively to purify therapeutic proteins. For this purpose a variety of chromatographic techniques are available based on different mode of operation and interaction chemistry. Among these techniques, ion exchange chromatography is the most widely used and accounts for many of the steps included in protein purification protocols in industrial production. As a result, ion exchange chromatography attracts a high amount of attention in scientific research aimed at optimizing the process. Optimization can be approached in many ways, including empirical, semi-empirical, and purely theoretical approaches. Empirical approaches are easy to implement. However, they require substantial amounts of time and materials and are not easily extrapolated to different conditions. Purely theoretical approaches also have limited value since we are still far from the level of knowledge required to accurately describe the complexity of separation problems in biotechnology. Therefore, semi-empirical approaches are preferred where mechanistic models are developed based on experimental data and used to predict process performance. The underlying mechanisms of protein adsorption equilibrium and transport vary dependent on the characteristics of the stationary phase and of the mobile phase. Thus, understanding how the process chemistry influences the process performance is absolutely necessary. This work focuses specifically on the effects of the counterion on protein adsorption equilibrium and kinetics in cation exchangers.

2. Background

Most scientific investigation starts with gathering background information in order to understand the basic known principles and the prior art in the field.

The scope of this chapter is to provide an introduction to chromatography in general, basis for separation in ion exchangers, and the main diffusion processes.

2.1. Chromatography in general

The use of chromatographic principles goes back to ancient times where already Aristoteles used clay to purify sea water. In the Bible, Moses is said to have thrown branches in the water to make it sweet, based on ion exchange properties of vegetable matter.

Generally, “chromatography” encompasses a variety of physico-chemical separation techniques, which have in common the selective distribution of a component between a mobile phase and a stationary phase. The different chromatographic techniques are categorized according to the interactions that are responsible for such selective distribution [1].

For example in size exclusion chromatography (SEC) the separating interaction is based on steric exclusion, where large molecules move faster through the stationary phase in contrary to small molecules which move slowly. Hydrophobic interaction and reversed phase chromatography (HIC & RPC) are depending on hydrophobic interactions, while separation in ion exchange chromatography (IEX) occurs due to electrostatic interaction. There would be a few more other chromatographic types to distinguish in liquid chromatography, but the mentioned ones are the most common ones [2].

Nowadays chromatography has become a widely used separation technique with a broad range of applications both at the analytical and at the process scale.

2.1.1. Chromatography in biopharmaceutical operations

In biopharmaceutical drug development chromatography is mostly used to get the desirable protein from the harvest broth into the medical formulation. This happens generally in three successive process steps: capture, purification and polishing. The first step is required due to low protein expression rates in fermentation, to reduce volume and to gain concentration. The second separates the target molecule from related impurities, while polishing is typically used to transfer the protein to its final formulation (stabilizing physiological buffer solution).

Industrial development in protein chromatography is mainly related to establishing the purification protocol in order to produce the required drug substance at the highest possible quality. The protocol is based on the three steps mentioned above and depending on the kind of product a specific set-up of chromatographic methods follows. After the purification protocol is completed at laboratory scale, it is transferred to pilot scale which is the intermediate between laboratory and production plant. In this step the purification protocol is optimized by simulating plant parameters and finally the whole purification process or so called downstream process is transferred to the production unit, where the biopharmaceutical drug substance is manufactured.

2.2. Cation exchange chromatography (CEX)

The basis for ion exchange chromatography (IEX) is the electrostatic interaction between the surface of the stationary phase and the molecules that are to be separated. In cation exchange chromatography (CEX), the stationary phase is negatively charged. Positively charged species can then be attracted and interact favorably, while negatively charged species are repelled. Thus, mixtures consisting of positively and negatively charged species can be easily resolved. Positively charged species can also be separated from each other using CEX when these species differ in the magnitude or spatial distribution of their charge. In this case, the strength of interaction varies from species to species allowing selective distribution and, hence, separation.

Typical IEX stationary phases, also called familiarly “resins”, consist of a backbone matrix functionalized with charged groups, which are called “ligands”. These ligands are responsible for the interaction with the mobile phase components. In CEX the ligands are negatively charged, while in anion exchange chromatography (AEX) the ligands are positively charged. Typical CEX ligands are carboxylic acid (C) and sulfopropyl acid (SP), while typical AEX ligands are diethylaminoethyl (DEAE) and quaternary ammonium ion (Q). C and DEAE are weak acid and weak base groups, respectively. Thus, these ligands carry charge only at intermediate pH values. Resins with such groups are called “weak”. Conversely, SP and Q ligands are strong acid and base, respectively, and are charged at any practical pH value. Resins with such ligands are called “strong”. It should be noted that the terms “weak” and “strong” do not indicate the protein binding strength, but merely whether the resin charge is pH dependent or not. In our work we use two CEX resins, UNOsphere S and Capto S, both with SP ligands but different matrix architecture [3].

2.2.1. Different types of cation exchange matrices

Many different matrix architectures are available. Polymer-based support matrices are very common. These can be based on either synthetic polymers or on natural polymers such as dextran, agarose and cellulose. Materials based on synthetic polymers typically possess rigid porous particles which are characterized by larger pores and higher mechanical strength but generally lower binding capacity [4]. Figure 1 shows a schematic drawing of a macroporous ion-exchanger particle.

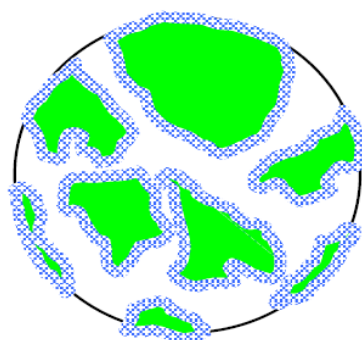


Figure 1: General pore structure of rigid porous materials [2]

UNOsphere S, used for the investigation in this work, is based on acrylamido and vinylic monomers with sulfonic acid ligands that are co-polymerized in the presence of a porogen to yields spherical beads with high porosity and relatively large pore sizes [5]. In contrast, media based on natural polymers are usually softer, with smaller pores and higher binding capacity, but generally with more modest flow properties [4].

Newly developed composite matrices combine the benefits of the high binding capacity of natural polymers with the mechanical strength of rigid macroporous media. These materials are obtained by incorporating a soft polymer within a more rigid support [3]. Figure 2 shows a schematic drawing of the composite material pore.

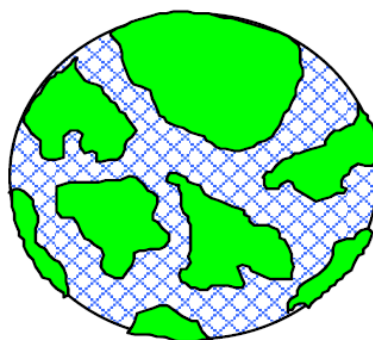


Figure 2: General pore structure of composite materials [2]

Capto S, the other cation exchanger used for the investigation of this work is an example of a composite matrix. Capto S consists of a highly cross-linked, rigid agarose backbone with grafted dextran polymers. In this case, the agarose matrix provides mechanical strength while the grafted dextran polymer, functionalized with SP-ligands, provides sites for protein binding [6].

2.3. Mass transfer effects

The performance of chromatographic processes depends, in general, on a variety of factors including flow non-uniformity in the column, hydrodynamic dispersion, and mass transfer kinetics. Flow non-uniformity across the column diameter can be avoided by proper packing and well-designed column headers. In practice, even very large-scale columns can be packed and operated with near plug flow conditions. For such columns, hydrodynamic dispersion and mass transfer determine performance. Their relative contribution varies dependent on the diameter of the chromatographic particles (d_p), the velocity at which the chromatographic process is operated (v) and the molecular diffusivity of the adsorbed component (D_0) [3]. The combined effects of these three parameters are expressed by the so-called reduced velocity (v'), which is given by:

$$v' = \frac{vd_p}{D_0} \quad (1)$$

As discussed in reference [3], when v' is small (less than about 20), hydrodynamic dispersion tends to be completely dominant while when v' is large (>100), mass transfer tends to be completely dominant. For applications of chromatography to process scale protein separations d_p and v are generally large. Moreover, because of their large molecular size, D_0 is small. As a result, v' for protein chromatography is usually very large (>1000) so that mass transfer tends to be the most significant effect and determinant of process performance. Thus, knowledge of the mass transfer kinetics is required to compare different stationary phases and predict process performance.

The kinetics of mass transfer is potentially influenced by two fundamentally different phenomena: external mass transfer and transport inside the particle [7].

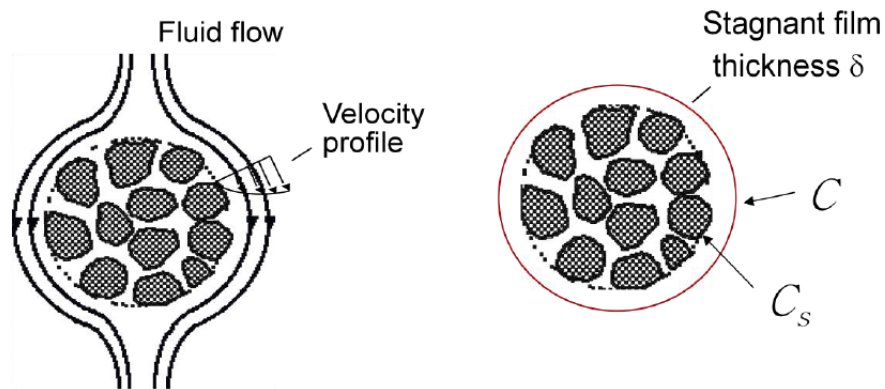


Figure 3: External mass transfer models [2]

External mass transfer is affected by fluid flow, while intra-particle transport is independent of the rate at which the mobile phase flows. Figure 3 shows schematically the external mass transfer in the fluid surrounding the particle. The actual flow path is extremely complicated. However, a simple model represents the external transport as if it were limited by diffusion across a stagnant film, whose thickness δ depends on the fluid flow. In this conceptual model, a higher fluid velocity leads to a smaller δ and thus to faster transport. In practice, the film thickness δ is very small, usually less than one tenth of the particle diameter. Thus, the external resistance to transport is usually very small [3].

On the other hand, transport inside the particle can be very slow. Since, in most cases, flow of the mobile phase does not occur inside the particles, intra-particle mass transfer is dependent on molecular diffusion. Two different mechanisms for diffusion can be considered: diffusion in the liquid-filled particle pores and diffusion in the adsorbed phase. The material characteristics of the stationary phase play a major role in determining which of these two mechanisms is likely to be responsible for intra-particle transport [3].

2.3.1. Pore diffusion

“Pore diffusion” occurs when the pores are large enough for the molecule to diffuse uninfluenced by the force field (electrostatic interactions in ion exchange) exerted by the pore wall. In this case, the driving force for mass transfer is the gradient in the solute concentration in the liquid phase. For the dilute conditions, typically encountered in protein chromatography (e.g. 1 g/L), this driving force is small and transport is slow [3]. Figure 4 shows a schematic of the pore diffusion process when a protein is strongly adsorbed at the pore wall.

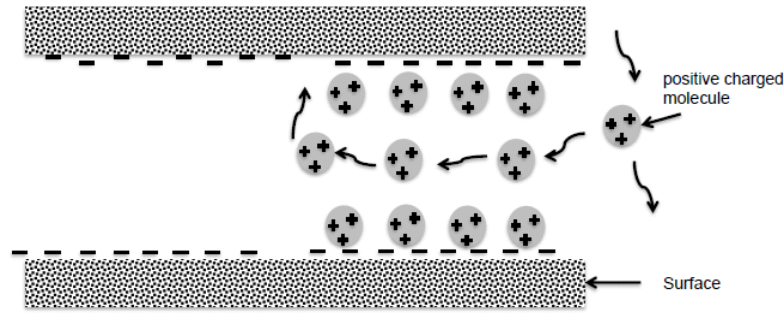


Figure 4: Schematic drawing of pore diffusion mechanism

In this case, Fick's law can be used to describe the protein flux in the stationary phase [3]. Accordingly,

$$J = -D_e \nabla c \quad (2)$$

where:

J = Protein mass transfer flux [$\text{g m}^{-2} \text{s}^{-1}$]

D_e = Protein effective diffusion coefficient in the stationary phase [$\text{cm}^2 \text{s}^{-1}$]

∇c = Protein concentration gradient [$\text{g cm}^{-3} \text{cm}^{-1}$]

The effective diffusivity D_e is introduced to account for the effect of porosity, tortuosity and hindrance. Accordingly, D_e is related to the molecular diffusivity D_0 by following equation [3]:

$$D_e = \frac{\varepsilon_p D_0}{\tau_p} \psi_p \quad (3)$$

where:

ε_p = Intra-particle porosity

τ_p = Tortuosity factor

ψ_p = Diffusional hindrance coefficient

The ε_p - term takes into account the restricted space available for pore diffusion within the particle, the τ_p -term considers the random orientation of the pores inside the particle, which provides an effective diffusion path that is longer than a straight way of movement. In general, τ_p is smaller for larger values of ε_p . However, it is best to regard τ_p as an empirical value, which should be determined experimental, for example by using a test solute which is not adsorbed. If τ_p once is measured for a test solute, the same value can be applied to other molecules as well as other system conditions. Usually, chromatographic resins show values of τ_p between 1.5 and 4 and between 0.6

and 0.8 for ε_p . Over-ranged values indicate severely restricted diffusion (for higher values) or that mechanisms other than pore diffusion are predominant in the measurement (for smaller values) [3].

In general the diffusional hindrance coefficient ψ_p , describes the ratio of protein and pore radii. Due to the fact that this ratio can be very high for proteins and other large biomolecules in chromatographic resins, diffusional hindrance needs to be especially considered. In common, for non-adsorbing types, two factors are engaged in ψ_p . The first one is entirely steric and related to size exclusion, which results from the fact that the centerline of the diffusing molecules cannot get to the pore wall at a distance closer than a molecular radius, whereas the second factor is associated with viscous drag or hydrodynamic resistance. Theories describing these factors are based on a colloidal representation of a protein molecule diffusing in an idealized cylindrical pore [3].

Since ε_p and ψ_p are both smaller than one and intra-particle porosity τ_p is larger than one, equation (3) gives $D_e \ll D_0$.

2.3.2. Solid diffusion

In the previous chapter pore diffusion was described where the transport of the protein takes place within the mobile-phase-filled particle. In contrast, “Solid diffusion” defines a mechanism where diffusion transport takes place in the adsorbed state within a phase which is different from the pore liquid. The solute concentration is generally similar in magnitude to the concentration in the external fluid. In the case of protein transport caused by pore diffusion the solute concentration and the concentration in the external fluid are almost equal, therefore the protein can as well attach to the pore surface as detach several times along its way through the particle. In the case of “Solid diffusion”, where protein adsorption is highly favorable, attachment can be permanent, but in both cases, only detached molecules undergo transport. However, the terms solid or surface diffusion and adsorbed phase diffusion are used to denote transport processes where diffusion occurs in the adsorbed state [3]. Figure 5 shows schematically the principle behind solid diffusion.

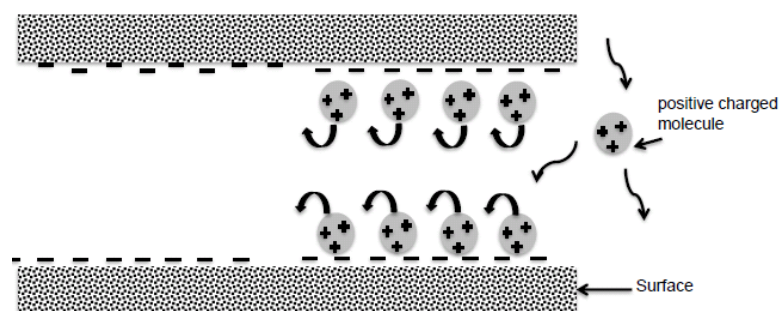


Figure 5: Schematic drawing of solid diffusion

Such processes are determined by surface diffusion which is associated with sliding along pore surfaces without detaching, micropore diffusion, related to the transport in cavities that are comparable in size to that of the diffusing molecule, and homogeneous diffusion, describing the transport in a pore filled with a liquid that is not mixable with the external fluid or the diffusion of a charged molecule in a contrary charged gel. Although the origin may be different for each of these mechanisms, they all are dependent on the same fact that the driving force for diffusion is a matter of the adsorbed-phase concentration, q . Accordingly, the mass transfer flux is given by [3]:

$$J = -D_s \nabla q \quad (4)$$

where ∇q is the concentration gradient in the adsorbed phase and D_s is the effective adsorbed-phase diffusivity. This equation is based on the same functional form as the equation for pore diffusion (2), however, there are major quantitative differences. Firstly, in general values for D_s are smaller than those of D_e since diffusion in the adsorbed phase is likely more limited. Secondly, D_s values are mostly concentration dependent, unlike values for pore diffusivities, which are typically independent of concentration, since the concentration in the adsorbed phase can be much higher than that in solution. Thirdly, when solid diffusion occurs by a “hopping” or “sliding” mechanism, it is likely that D_s depends on the binding strength, approaching vanishingly small values when the solute is very tightly held by the surface, but increasing as binding becomes weaker. Finally, depending on the given conditions the magnitude of the diffusion flux can be quite varying. If a high capacity adsorbent is given, q can be much larger than C , even if D_e is bigger than D_s , the mass transfer flux in the adsorbed phase may be much larger than that coming from pore diffusion [3].

In the case of gas adsorption, surface and micropore diffusion mechanisms are well proven for many practical materials reaching from zeolites to activated carbon. Also well investigated is the homogeneous diffusion of ions in cross-linked ion exchange resins, including organic ions like amino acids. However, diffusion mechanisms in the adsorbed phase of proteins are far less well understood. Difficulties in understanding, rely on the fact that mass transfer models based on vastly different transport mechanisms, generally supply similar descriptions of macroscopic adsorption rate data [3].

2.4. Counter diffusion (Nernst-Planck effect)

In IUPAC Compendium of chemical terminology the counter-ion is described as the mobile exchangeable ion in ion exchangers [8]. This means, that if an ion exchange resin, for example a cation exchange resin (negative charged ligands), is equilibrated with sodium-chloride buffer, the positive charged sodium-ion will be bound by the surface ligands of the cation exchanger. When a molecule with a higher binding affinity than that of the bounded counter-ion is introduced (e.g. the protein), the counter-ion is replaced by this molecule.

In the previous two chapters the diffusion process of proteins was described by means of the Fickian diffusion equation. For electrolytes, however diffusional transport is more appropriately treated with the Nernst-Planck equation, which takes into account the effect of the diffusion- induced electric field on the diffusion flux [9].

The Nernst-Planck equation is an extension of Fick's law for the description of counter-ion diffusion, where the driving force is the electrochemical potential gradient instead of the concentration gradient. The diffusion flux of an ionic species i is given by the Nernst-Planck equation as follows:

$$J_i = D_{p,i} \left[\nabla c_{p,i} + \frac{z_i F}{RT} c_{p,i} \nabla \Phi_p \right] \quad (5)$$

where:

J_i = Diffusion flux of species i through the stagnant film around the particle

$D_{p,i}$ = Diffusion coefficient of species i

$\nabla c_{p,i}$ = Concentration gradient of species i in the particle

z_i = Charge on species i

F = Faraday constant

Φ_p = Electrical potential in the particle

The first term describes the flux caused by the concentration gradient, while the second term describes the electrophoretic motion of the ion in an electric field. Note that c_p can be replaced by either c or q and D_p by either D_e or D_s dependent on whether pore or solid diffusion is dominant, respectively.

As shown by Helfferich [10], the Nernst-Planck equation predicts that the diffusion fluxes of all charged species are coupled by the common electrical potential gradient. Because of this coupling, when two counter-ions having different diffusivity are exchanged, an electrical potential gradient is established. This gradient slows down the

fast counter-ion by speeds up the slow one. This effect is most pronounced when the difference in diffusivity is very large, which is expected to be the case when a bulky protein is exchanged for a faster diffusing counter-ion. For a given protein, the magnitude of this effect can be expected to be more significant for a smaller faster diffusing counter-ion than for a bulky one and for counter-ions of smaller charge.

3. Goals and objectives

The objective of this work is to investigate the effects of the counterion type on the adsorption of proteins in two types of ion-exchangers with different pore structures. UNOsphere S, which features a macroporous architecture, and Capto S, which has a much smaller pore size due to charged dextran grafts on an agarose-based matrix. Although the basic electrostatic interaction of the protein with the adsorbent is essentially the same for both materials, the pore structure is expected to have a profound influence on the adsorption kinetics. Several research studies were done to gain a better understanding of diffusion principles inside these materials. Whereby protein diffusion in macroporous materials is fairly well understood, there are still many unanswered questions regarding transport in dextran-grafted matrices like Capto S, where protein diffusion occurs in close proximity to the charged ligands, rather than in open macropores.

A potentially important effect that has yet to be elucidated, is that of the type of counterion on the adsorption kinetics in these materials. It is well known that, in general, diffusion of counterion is coupled according to the Nernst-Planck equations. However, it is unknown to what extent this is a factor in protein adsorption. The effect of protein binding strength is also unknown. Binding strength is also likely to be affected by the counterion type. In turn this could affect the mobility of adsorbed protein molecules and, thus, adsorption kinetics.

In this regard two different hypotheses are advanced. The first hypothesis postulates that protein transport in Capto S is enhanced by electrostatic coupling of the diffusion fluxes between the fast diffusing counterions and the slow diffusing protein. This leads to the fact that the coupled diffusion (of counterion and protein) forces the two components to diffuse at the same rate, which means that the slower species is speeded up and the faster one slowed down [9]. In this connection, electrostatic coupling is described by the Nernst-Planck equations, which predicts an electrical potential gradient induced by the different diffusional mobility of the exchanging counter-ions.

The second hypothesis postulates that protein transport is enhanced by a solid diffusion mechanism driven by a large adsorbed concentration driving force and by mobility in the adsorbed phase which in turn, depends on the binding strength. Accordingly, we postulate that if protein binding is not too strong, protein molecules can hop from one adsorption site to another. This hypothesis has been introduced by Lenhoff in 2008 [11] to describe the effect of ionic strength on protein adsorption in certain cation exchangers.

In order to validate these hypotheses several experiments will be done using lysozyme as a model protein. Isotherms will be determined at low salt concentrations to determine the protein equilibrium binding capacity; batch uptake curves will be obtained to gain the effective diffusivity of the protein; and linear gradient elution experiments will be performed to determine protein binding strength and binding charge [7].

Based on their molecular properties, four different ions were chosen for this work: sodium, which is a small monovalent counterion; calcium which is a small bivalent counterion; and arginine and tetra butyl ammoniumhydroxide which are two bulky monovalent counterions. Since the ionic mobility and the electrostatic coupling effects predicted by the Nernst-Planck equations are different for these different counter-ions, the results should show whether diffusional flux coupling or binding strength affect protein adsorption rates in Capto S.

For UNOsphere S no significant effects are expected because the controlling adsorption mechanism is likely to be pore diffusion. In this case, the protein concentration in the pore fluid is expected to be too low to give significant flux coupling. The proposed approach is to determine the batch adsorption kinetics for the different counterions and express the results in terms of effective pore diffusivities D_e . Protein binding strengths will also be determined for each counterion. It will then be determined based on the experimental trends whether the D_e -values are correlated with the counterion properties according to the Nernst-Planck model or with protein binding strength according to the hopping model.

As another objective of this work I want to mention my personal goal for this work. The performance of the experiments which the results of this work are based on should lead to an improvement of my prior knowledge in chromatography. Furthermore this work provides practical entry to the investigation of diffusion processes in biomolecular separation and the related basic theoretical background.

4. Experimental techniques

4.1. Materials

Proper interpretation of the experimental results obtained in this work requires knowledge of the material properties of the resins used. Moreover, for the interpretation of the results the characteristics of the model protein and the different counterions are needed.

The experimental work was conducted with two different types of cation exchangers. UNOsphere S, which consists of rigid macroporous polymer based particles, and Capto S, which is a crosslinked agarose matrix with charged dextran polymer grafts.

4.1.1. Particlesizedistributions

The particle size has a pronounced effect on mass transfer kinetics. Thus, it is important to know the distribution of sizes and the average particle size, in order to interpret the experimental kinetics results [3].

Particle size distributions were obtained by Tao [4] and are shown in Figure 6.

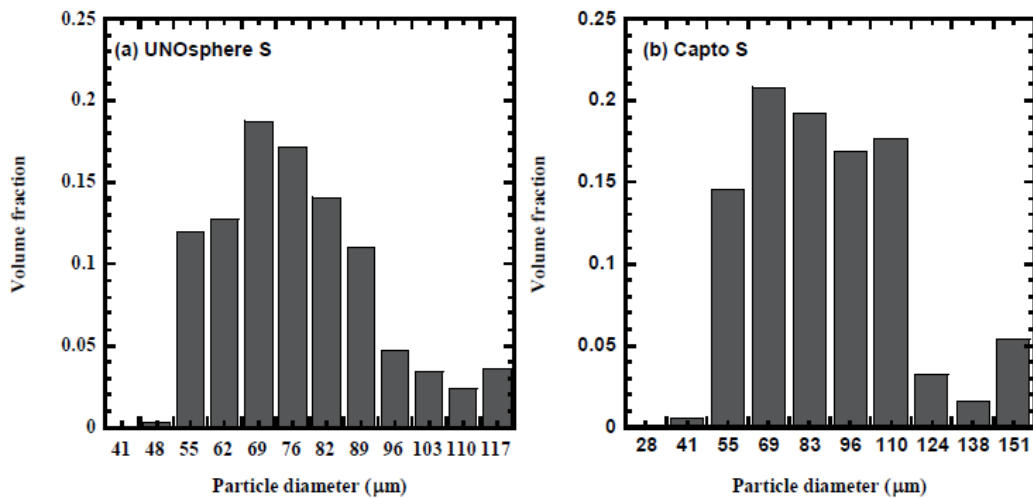


Figure 6: Particle size distribution for (a) UNOsphere S and (b) Capto [4]

Based on the particle size distribution the average particle size \bar{r}_p was determined (see table 1). This was used to determine the effective diffusivity from batch uptake experiments following the procedure outlined in reference [3].

4.1.2. Properties of the stationary phase

Table 1 summarizes the relevant physical and chemical properties of the materials used in this work as determined by Tao [4].

Table 1: Summary of stationary phase properties [4]

Matrix	q_0 ($\mu\text{mol/ml}$)	\bar{d}_p (μm)	ε	$\varepsilon_p^{(3)}$	$\varepsilon_{pM}^{(3)}$	r_{pore} (nm) in 0 M NaCl ⁽⁴⁾	r_{pore} (nm) in 1 M NaCl ⁽⁴⁾
UNOsphere S	148	75	0.33 ⁽¹⁾	0.80	0.58	68±20	74±20
Capto S	220	89	0.37 ⁽²⁾	0.74	ND	ND	ND

⁽¹⁾ based on pressure drop and Karman-Cozeny equation in 0 M NaCl

⁽²⁾ based on retention of blue dextran

⁽³⁾ based on retention of glucose

⁽⁴⁾ based on dextran exclusion

q_0 is the charge density, which is the concentration of charged ligands. ε is the extra-particle porosity in packed columns, ε_p is the intra-particle porosity accessible by glucose, and ε_{pM} is the intra-particle macroporosity. r_{pore} is the average pore radius determined by inverse size exclusion chromatography (iSEC) in 0 and 1 M NaCl. Note that the r_{pore} values were not determined for Capto S since this material excludes the neutral macromolecules used for iSEC because of the presence of the dextran grafts [4].

4.1.3. Lysozyme as model protein

Lysozyme (from chicken egg white, Sigma-Aldrich, St. Louis, MO, USA) was used as model protein in this work, because its structure and biochemical behavior are well known.

Its diffusivity in free solution is $D_0 = 11.4 \times 10^{-7} \text{ cm}^2/\text{s}$ [12] and its net charge dependence on pH is shown in Figure 7.

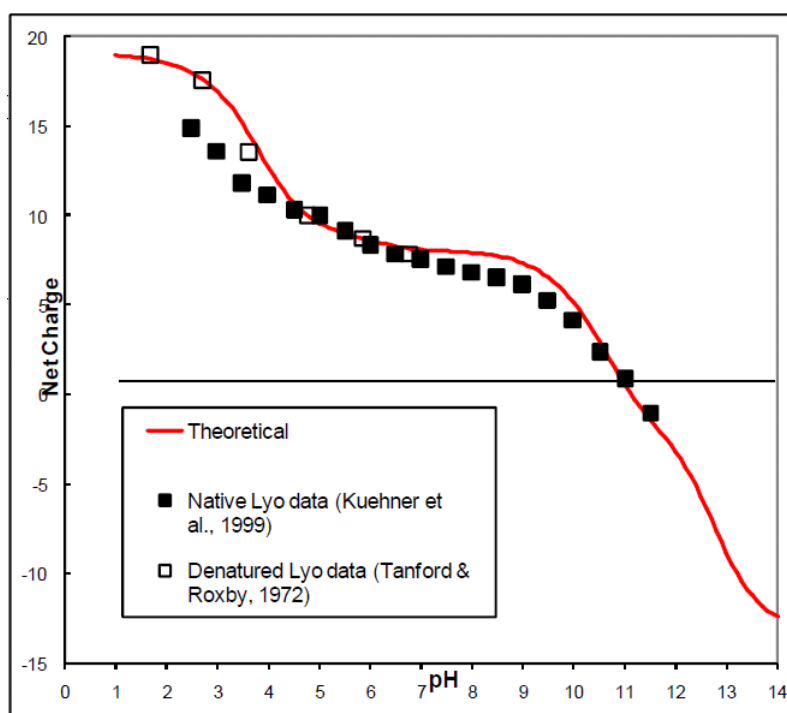


Figure 7: Lysozyme - Net charge vs. pH [2]

The net charge is a critical parameter in the adsorption behavior of proteins on ion exchangers. Since our work involves CEX, the protein should be positively charged. Thus, a pH of 5.0 is used for this work. From Figure 7, at this pH lysozyme has a net charge of +8 and is expected to bind strongly to the two CEX resins chosen.

The hydrodynamic radius of lysozyme is around 1.9 nm [12], which compared to the pore size of UNOsphere S (see Table 1) is several times smaller. This is a very important requirement for pore diffusion, where the pore size of the resin particle has to be at least 5 times larger than the size of the protein.

Figure 8 shows the molecular structure of lysozyme with a size of 2.6 x 4.5nm. It is an ellipsoid shaped molecule, molecular mass is 14.7kDa; the mass density is 1.37g/cm³.

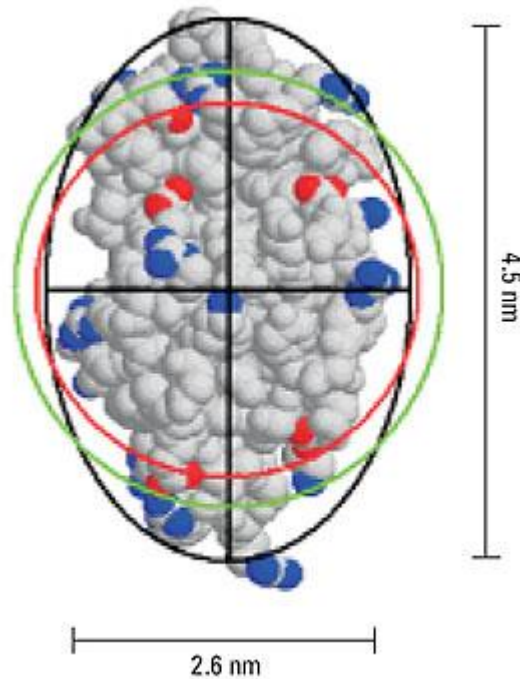


Figure 8: Lysozyme - molecular structure [3]

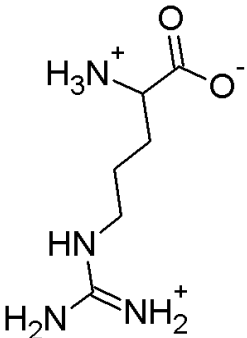
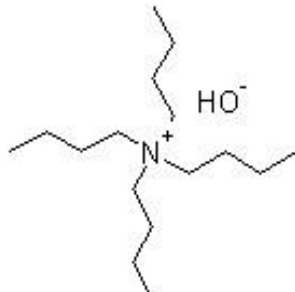
Lysozyme is also known as muramidase or N-acetylmuramide glycanhydrolase. It belongs to the glycoside hydrolases, enzymes which damages bacterial cell walls by catalyzing hydrolysis of 1,4-beta-linkages between N-acetylmuramic acid and N-acetyl-D-glucosamine residues in a peptidoglycan and between N-acetyl-D-glucosamine residues in chitodextrins. Lysozyme is abundant in a number of secretions, for example in human milk. It is also present in cytoplasmic granules of the polymorphonuclear neutrophils (PMN). Large amounts of lysozyme can be found in egg white. C-type lysozymes are closely related to alpha-lactalbumin in sequence and structure, making them part of the same family. In humans, the lysozyme enzyme is encoded by the *LYZ* gene.

The molecular, three-dimensional structure (as shown in figure 8) was described in 1965 via X-ray crystallography. Lysozyme was the second protein structure and the first enzyme structure to be solved via X-ray diffraction methods, and the first enzyme to be fully sequenced that contains all twenty essential amino acids. Furthermore, it was also the first enzyme to have a detailed, specific mechanism suggested for its method of catalytic action [12].

4.1.4. Counterion properties

To test the influence of different counterions on the adsorption of proteins, four different types of cations were used, which are shown in Table 2 along with their molecular diffusivities.

Table 2: Species of counterions and their respective diffusivity values

Counterion	Diffusivity (cm ² /s)
Na ⁺	1.3×10^{-5}
Ca ²⁺	0.79×10^{-5}
Arginine (C ₆ H ₁₄ N ₄ O ₂) 	$*6.0 \times 10^{-6}$
Tetrabutylammonium hydroxide (C ₁₆ H ₃₇ NO) 	$*4.2 \times 10^{-6}$

[^] Diffusion Mass Transfer in Fluid Systems E.L. Cussler, Diffusion – Mass Transfer in Fluid Systems, 2009, 3rd edition.

* Calculated from Wilke-Chang with LeBas addition volumes as outlined in Sherwood, Pigford, and Wilke, Mass Transfer, McGraw-Hill, 2009

Table 2 shows that arginine and TBAH have lower diffusivities due to their larger molecular size.

Sodium and calcium have almost identical atom radii (180pm, empirical calculated) [13], therefore if calcium shows an influence on the adsorption it should be due to its bivalent charge.

Raw substances for buffer preparation obtained from Fisher Scientific (Pittsburg, PA, USA):

- Calcium acetate monohydrate (100%)
- Sodium acetate (100%)
- Arginine free base (100%)
- Tetrabutylammonium hydroxide (1M stock solution)

Buffer corresponding to each type of counterion were prepared as follows:

- Required amount of raw substance or stock solution was diluted with deionized water, pH adjusted with concentrated acetic acid (pH 5.0), filled up to the final volume and filtrated through 0.45 μm membrane filter.

4.2. Adsorption isotherms

Adsorption is generally defined as the concentration of an adsorbate species at a solid surface. Protein adsorption is influenced strongly by the specific biomolecular properties. Thus adsorption of proteins is generally much more complicated because of their inherent complexity. These properties include the heterogeneous distribution of charged and hydrophobic groups of the protein, the varying structure of the protein (the structure of bonded proteins can be different from proteins in solution), the dominant influence of ionic strength on the protein diffusion behavior, aggregation due to the protein molecules tendency to self-associate and slow adsorption rates because of limitation in binding kinetics [3]. Therefore an experimental determination of adsorption isotherms, where the concentration of adsorbed protein in the stationary phase at equilibrium with the mobile phase is measured, is needed.

In this work, experimental adsorption isotherms were obtained by suspending different amounts of resin particles in appropriate volumes of protein solution, each sample having a known initial protein concentration. The samples were equilibrated in test tubes gently rotated end-over-end for at least 24 hours at room temperature and then allowed to settle. The supernatant protein solution was then sampled and tested with a Nanovue (GE Healthcare, Piscataway, NJ, USA) spectrophotometer to obtain the absorbance at 280nm. This absorbance was then used to calculate the residual concentration of protein in solution using a calibration curve at the same wavelength. Hence, the concentration in the adsorbed phase was calculated from a mass balance and the adsorbed protein concentration q was plotted versus the residual concentration of protein in solution.

The general, the isotherm is expected to be in a linear correlation between adsorbed protein and protein in the mobile phase in the low concentration range. In practice, this is difficult to observe under conditions where protein adsorption occurs very fast. Therefore in many case the relationship is highly non-linear and levels off to a maximum capacity. However, under a high salt concentration a linear relationship is expected because binding is weaker. The linear isotherm limit is based on the concentration of accessible binding sites and on the specific affinity of the protein for these sites. In contrast, the maximum capacity is mostly limited by the accessible surface area or by the concentration of binding sites [3].

To describe the protein adsorption equilibrium a theoretical adsorption isotherm is often used. Two frequently used expressions are the *Langmuir isotherm* and the *steric mass action (SMA) model* [7].

4.2.1. The Langmuir Model

The Langmuir model was used in this work to fit the experimental data. Originally developed for the adsorption of gases onto metal surfaces the Langmuir theory is based on a kinetic principle, in which the rate of adsorption is assumed to be equal to the rate of desorption from the surface [14]. It can be described by following equation:

$$q = \frac{q_m KC}{1+KC} \quad (6)$$

Where q (kg/m^3) is the adsorbed protein concentration, q_m (kg/m^3) the monolayer capacity, K represents the equilibrium constant (ratio of forward and reverse rate constants for adsorption and desorption) and C the protein concentration in the mobile phase (kg/m^3) [3].

4.2.2. The steric mass action model

The SMA model considered explicitly the exchange of counterions and takes into account the shielding of charges on the adsorbent surface by the adsorbed protein. The underlying assumption is that protein adsorption occurs via the stoichiometric exchange with counterions according to the mass action law principle (MA) [15]. The steric mass action model (SMA), introduced by Brooks and Cramer [16] is an important refinement of the MA model. Figure 8 illustrates the underlying concept.

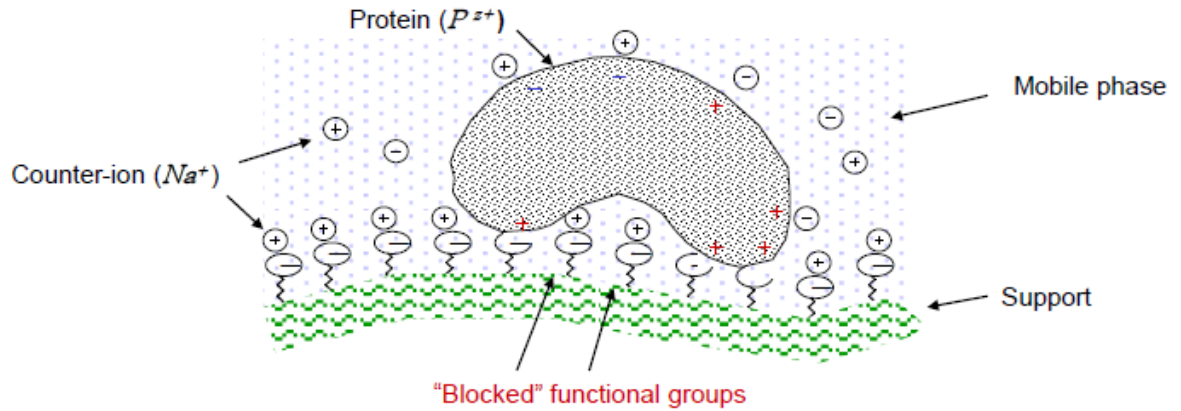


Figure 9: Drawing of the steric mass action model [2]

The key assumption of the SMA model is that because of the large footprint of the protein molecule, the binding of the protein not only involves z -ligands through a counterion exchange process as in the MA model, but also results in the shielding or blocking of a number σ of these ligands [3].

The SMA model is given by the following isotherm expression [3]:

$$q = \frac{K_e [q_0 - (z + \sigma)q]^z C}{(C_{Na^+})^z} \quad (7)$$

where:

q = Adsorbed protein concentration [kg/m^3]

q_0 = Concentration of charge ligands in the stationary phase [mol/m^3]

z = Protein effective charge

C = Protein concentration in mobile phase [kg/m^3]

K_e = Equilibrium constant for ion exchange

C_{Na^+} = Counterion concentration (e.i. Sodium) [kg/m^3]

σ = Steric hindrance or shielding factor

The Langmuir and SMA models describe similarly shaped adsorption isotherms. However, an advantage of the SMA model is that it describes explicitly the dependence of binding on counterion concentration. The SMA model was not applied in this work for fitting the isotherm data since isotherms were obtained only at a single counterion concentration (20mM and 10mM). However, the SMA model was used in this work to

analyze the results of linear gradient elution experiments (LGE) which spanned a range of counterion concentrations. These results were used to determine the binding strength as measured by the slope of the linear isotherm.

4.3. Linear gradient elution

Gradient elution in general means that the composition of the mobile phase modifier (e.g. sodium acetate, in our case) changes over time. The modifier travels ahead of the feed component (protein), due to the fact that the modifier has a lower affinity to the stationary phase in comparison to the protein. Thus, the interaction (retention or elution) of the protein with the stationary phase depends on the local concentration of the modifier in the mobile phase at each point in the column and at each point in time. By measuring the slope of the isotherm, the binding strength with different counterions (mobile phase modifier) can be determined [3].

In principle, this information is contained in the isotherm data as given by the initial slope of the isotherm in the so-called Henry's law region. However, in practice, because of the very favorable binding, the initial slope of the isotherm could not be determined with any accuracy. Linear gradient elution (LGE) experiments carried out in the Henry's law region were thus done for this purpose according to following procedure [3]:

A Tricorn-column (0,5cm diameter, 3,2cm long) from GE Healthcare was packed with the stationary phase and connected to an AKTA Explorer 10 unit also from GE Healthcare. The column was first equilibrated with buffer corresponding to each counterion at initial concentration (20mM in general and 10 and 20 mM for calcium acetate) at a flow rate of 0,5 mL/min, until the effluent from the column showed constant conductivity. The lysozyme sample was loaded onto the column in a volume of 50 μ L. After loading, the concentration of the mobile phase modifier was increased gradually with varying gradient slopes while keeping a constant flow rate of 0,5 mL/min. UV absorption at 280nm and conductivity were recorded in order to determine the conductivity at which lysozyme eluted for each counterion type. The corresponding buffer was calculated from the conductivity using the experimentally determined relationship between conductivity and buffer concentration. For this purpose each counterion buffer conductivity was measured at different concentrations and a polynomial correlation was used to regress the data. The concentration of the counterion at which the protein elutes was calculated from the polynomial fit. With the calculated concentration, the analysis of the experimental results for each gradient slope is based on following (summarized) procedure:

1) The normalized gradient slope γ was calculated from the following equation:

$$\gamma = \frac{\beta L}{v} \quad (8)$$

where:

β = gradient slope [mM/s] or [mM/m³]

L = Column length [m]

v = Interstitial velocity of mobile phase ($=u/\epsilon$) [m/s]

2) γ was plotted (logarithmic scale) versus the concentration of the counterion at which the protein elutes C_M^R as is shown schematically in Figure 9.

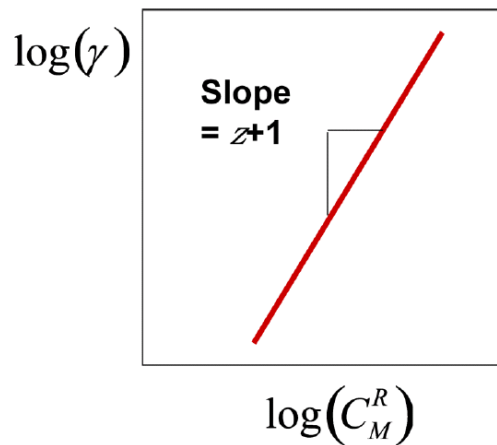


Figure 10: LGE relationship for ion exchange chromatography [2]

3) The following equation obtained from the SMA model as discussed in ref. [3] was then used to determine the protein effective binding charge, z , and equilibrium binding parameter, A_i :

$$C_{M,i} = [A_i (z_i + 1) \gamma]^{\frac{1}{z_i + 1}} \quad (9)$$

where:

$C_{M,i}$ = Concentration of the modifier (counterion) at which protein elutes

A_i = Equilibrium parameter for retention in IEX (referred to protein-counterion exchange)

z_i = Effective charge of the protein

Thus, z and A can be obtained from the slope and intercept of the plot in Figure 9. After these parameters are obtained, the protein retention factor k' is obtained as a function of salt concentration from the following equation:

$$k' = k'_M + AC_M^z \quad (10)$$

where k'_M is the retention factor of the salt. Finally, k' is related to the slope of the binding isotherm K by the equation:

$$k' = \phi K \quad (11)$$

For the experimental performance, following setup was chosen:

- Experiments were only conducted on Capto S, using the “Äkta-Explorer” chromatography station.
- Runs for sodium acetate were done with a start concentration of 20mM sodium acetate pH 5 to a final concentration of 1000mM sodium acetate pH 5. Four different gradient slopes were tested → 20mM NaAc to 1000mM in 5/10/20/30 column volumes. The same was done for calcium acetate, beside the fact that initial concentration was 10mM calcium acetate pH 5 (accordingly to sodium, calcium is bivalent → half concentration)
- LGE for arginine pH 5 was done with an initial concentration of 15mM arginine to a final concentration of 750mM arginine because of limited amount of arginine raw substance. Gradient slopes were the same like for sodium and calcium (15mM arginine to 750mM arginine in 5/10/20/30 column volumes)
- LGE for TBAH pH 5 was done starting at 20mM TBAH pH 5 to 750mM TBAH pH 5 in 5/10/20/30 column volumes. Final concentration of TBAH at 750mM was chosen due to limited amount of TBAH raw substance (buffer was made out of 1M stock solution).
- System setup: overall flow rate → 0.5 ml/min; column dimension: 0.5 cm diameter / 3.2 cm length / 1 CV = 0.628 ml
- Sample: 2g Lysozyme/ L solution → Injection volume: 50µl

4.4. Batch uptakes kinetics

The batch uptake kinetics of lysozyme was determined with a stirred-batch apparatus on UNOsphere S and Capto S with different counterions. In each case, excess liquid was first removed from the resin by centrifugation (2 x 5min at 5000 rpm) and a known amount of centrifuged resin particles was suspended in 20ml of protein solution, containing 1mg/ml lysozyme.

While under constant agitation with a small paddle stirrer, the solution was circulated with a peristaltic pump through a UV detector, which measured the 280 nm absorbance of the solution. The technical flow scheme of the apparatus is shown in Figure 10.

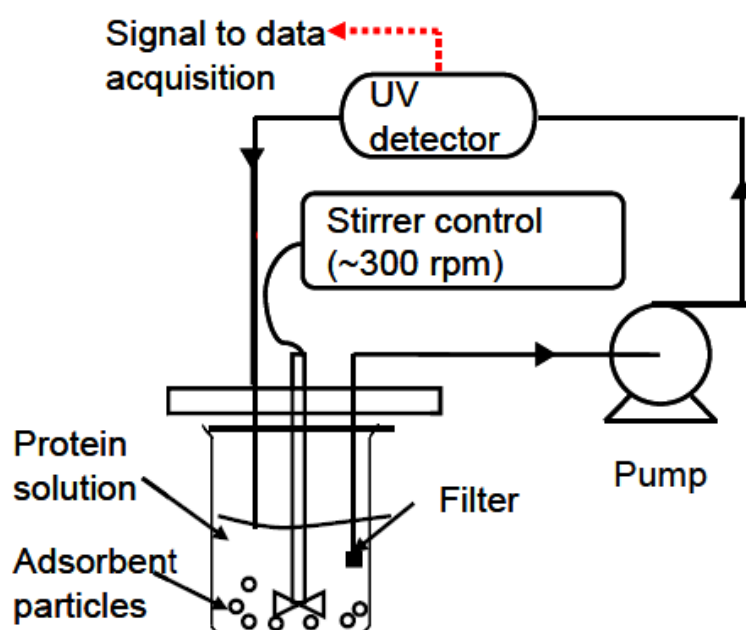


Figure 11: Flow scheme of the batch uptake apparatus [4]

Before adding the resin sample to the vessel, the UV absorption of both the buffer and the protein solution were measured and the values used to construct a calibration curve which was then used to convert the UV absorbance readings to protein concentration. In these experiments, the protein concentration varies as a function of time and the amount of protein adsorbed at each time per unit particle volume is obtained by material balance.

Accordingly,

$$\bar{q} = \frac{V}{V_M} (C_0 - C) \quad (12)$$

where \bar{q} is the particle-average adsorbed protein concentration, V the volume of the sample solution, V_M the volume of the particles, C the protein concentration in the fluid phase (mg/ml) and C_0 the protein concentration in the initial fluid phase (mg/ml).

To minimize the experimental error, the ratio V/V_M was adjusted in such a way that the change in protein solution concentration over time was substantial declining to about one half of the initial value.

Batch adsorption methods are suitable for measuring mass transfer rates with nonlinear isotherms and at high adsorbate loadings. For the interpretation of the results, models taking into account the time-varying concentration are required. Therefore an analytical solution of a model assuming that pore diffusion is controlling and taking into account the averaged particle size was used to describe the uptake curve [7]. The effective diffusivity was obtained by comparing the experimental uptake curves with those calculated from this model.

5. Results and discussion

5.1. Adsorption isotherms

Adsorption isotherms were obtained for both resins at 20mM sodium acetate pH5, 20mM arginine pH5, 20mM calcium acetate pH5, 10mM calcium acetate pH5, and 20mM TBAH.

Most of the isotherms were performed with 10 measurement points, but some have only 9 because of mistakes in sample preparation (dilution errors).

Markers represent measurement points while curves are based on the Langmuir model fitted to the data.

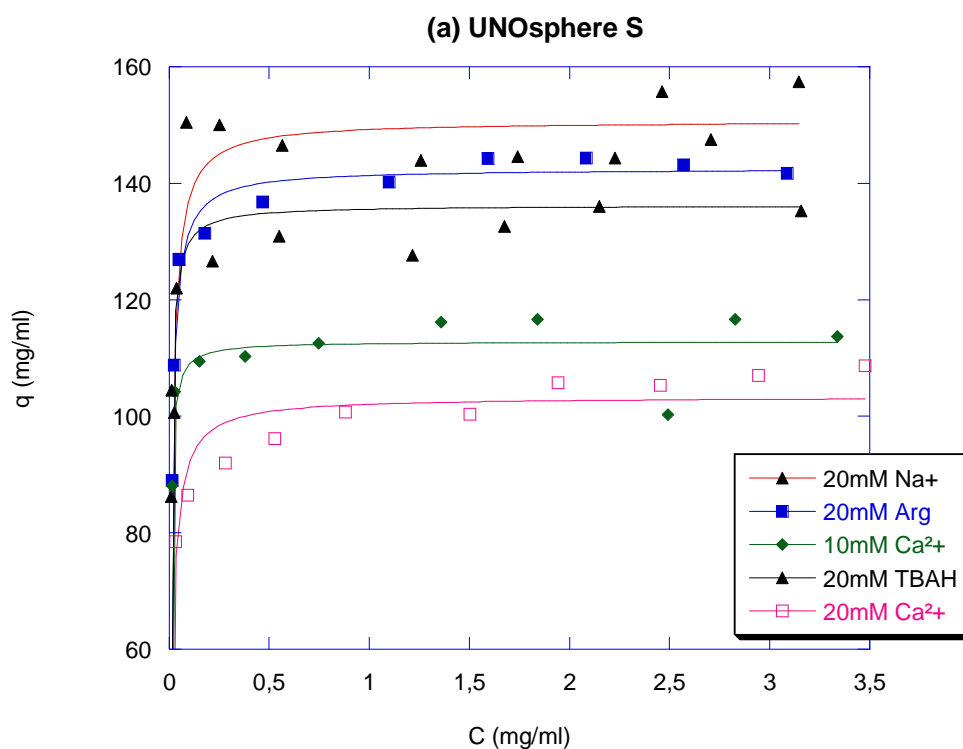


Figure 12: Adsorption isotherms on UNOsphere S

Adsorption isotherms for UNOsphere S are summarized in figure 11. Curves based on the Langmuir isotherm (chapter 4.2.1) are shown to correlate the data

The maximum lysozyme binding capacities (at equilibrium) determined for UNOsphere S are summarized in Table 3.

Table 3: Summary of maximum lysozyme binding capacities for UNOsphere S

UNOsphere S	
Counterion	q [mg/ml particle]
20mM Na ⁺	149
20mM Arginine	141
20mM Ca ²⁺	103
10mM Ca ²⁺	112
20mM TBAH	136

Previous studies [5] have shown a lysozyme binding capacity of 150 mg lysozyme/ml particle in 20mM sodium buffer at pH 5. Therefore the results obtained in this work seem to be consistent. Arginine and TBAH show results similar to sodium with the differences likely stemming from experimental variance. However, the lysozyme binding capacity in the calcium buffers is definitely lower whether the comparison is made at the same molar concentration (20mM calcium) or at the same equivalent concentration (10mM calcium) as for sodium, arginine, and TBAH. This result suggests that the lysozyme-calcium exchange equilibrium is less favorable than the exchange with monovalent counterions, resulting in less protein binding.

Figure 12 shows the isotherms for lysozyme on Capto S, comparing the different counterions (overall buffer condition was pH5). Like in the case of UNOsphere S, curves based on the Langmuir isotherm (chapter 4.2.1) are shown to correlate the data.

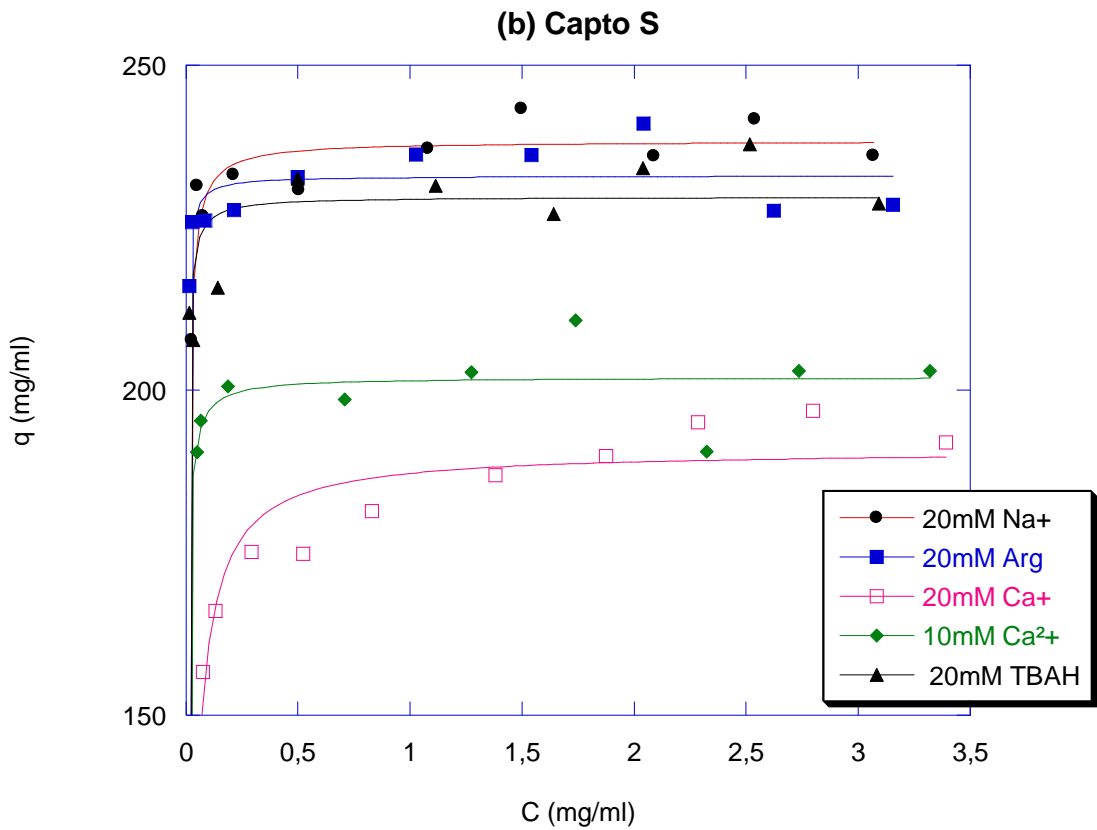


Figure 13: Adsorption isotherms on Capto S

Table 4 summarizes the binding capacity at equilibrium for Capto S obtained from adsorption isotherms (Figure 12).

Table 4: Summary of isotherm results on Capto S

Capto S	
Counterion	q [mg/ml particle]
20mM Na ⁺	237
20mM Arginine	232
20mM Ca ²⁺	191
10mM Ca ²⁺	201
20mM TBAH	230

The trends with regards to counterion type are similar to those observed for UNOsphere S with the calcium buffers exhibiting the lowest protein binding capacity. The discrepancy between TBAH, arginine and sodium is also within the experimental variance. In general it is shown that Capto S has a higher capacity at equilibrium than UNOsphere S.

As an issue of experimental performance it should be mentioned that this isotherm measurement method is very sensitive due to the fact that results are strongly dependent on accurate concentration determination. Therefore a careful handling is required.

5.2. LGE

The chromatographic LGE-peaks for each counterion are summarized in figure 12 for sodium, figure 13 for calcium acetate and figure 14 for arginine. Results for TBAH (figure 19) were not analyzed due to fact that lysozyme was eluting in all cases at the end of the gradient (750mM), where no meaningful evaluation is possible.

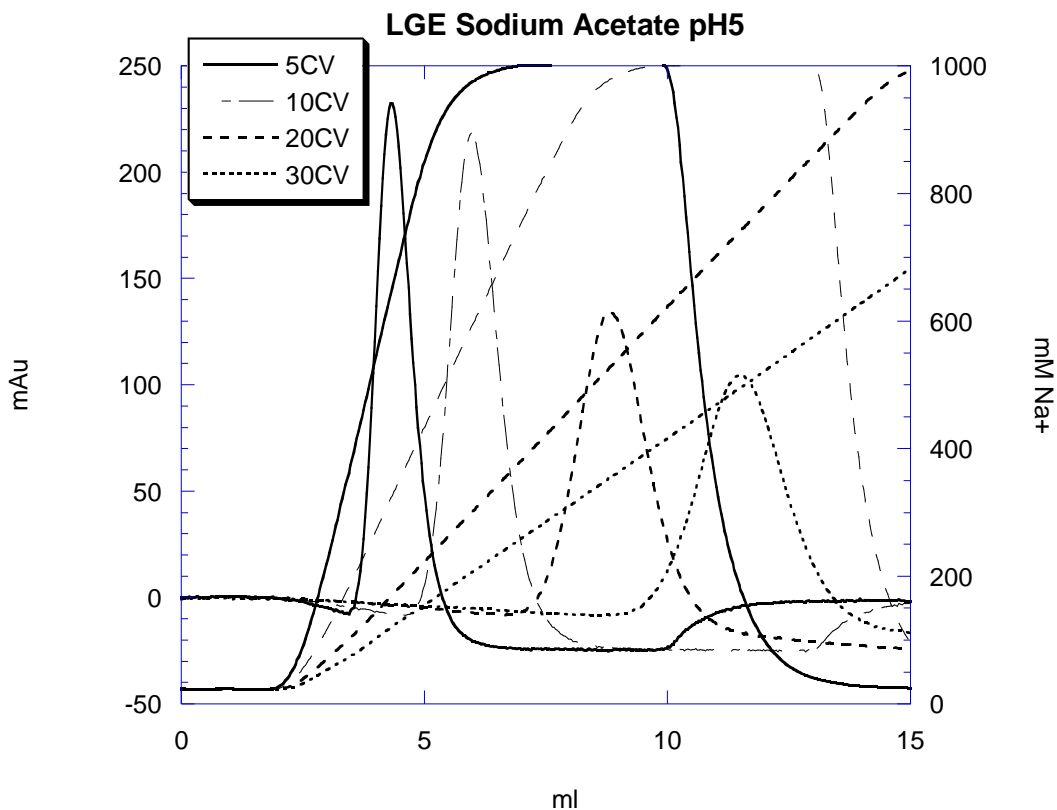


Figure 14: LGE chromatographic peaks for sodium

As it is shown in the results for sodium acetate at pH 5, the concentration of sodium at which the protein elutes increases as the slope of the gradient gets steeper. Furthermore the fact that at a lower slope of the gradient leads to a higher peak width can be observed, which is applied in separation of two component systems (i.e. a protein which needs to be purified from impurities) to achieve a higher resolution and hence better separation.

LGE curves for calcium acetate pH 5 (Figure 14) look similar to sodium, beside that the initial gradient concentration was at 10mM instead of 20mM. However, as the gradient slope gets steeper, the concentration at which the protein elutes becomes higher.

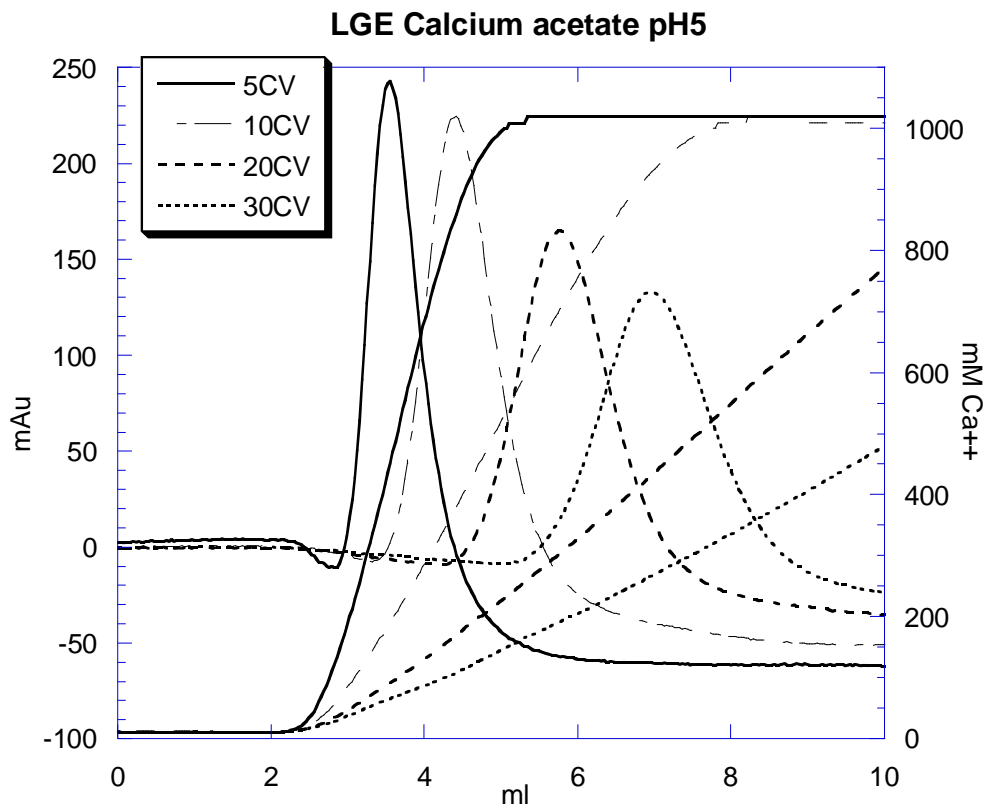


Figure 15: LGE chromatographic peaks for calcium

Elution profiles obtained from LGE for arginine at pH are shown in Figure 15, initial gradient concentration was at 15mM to a final concentration of 750mM arginine pH 5.

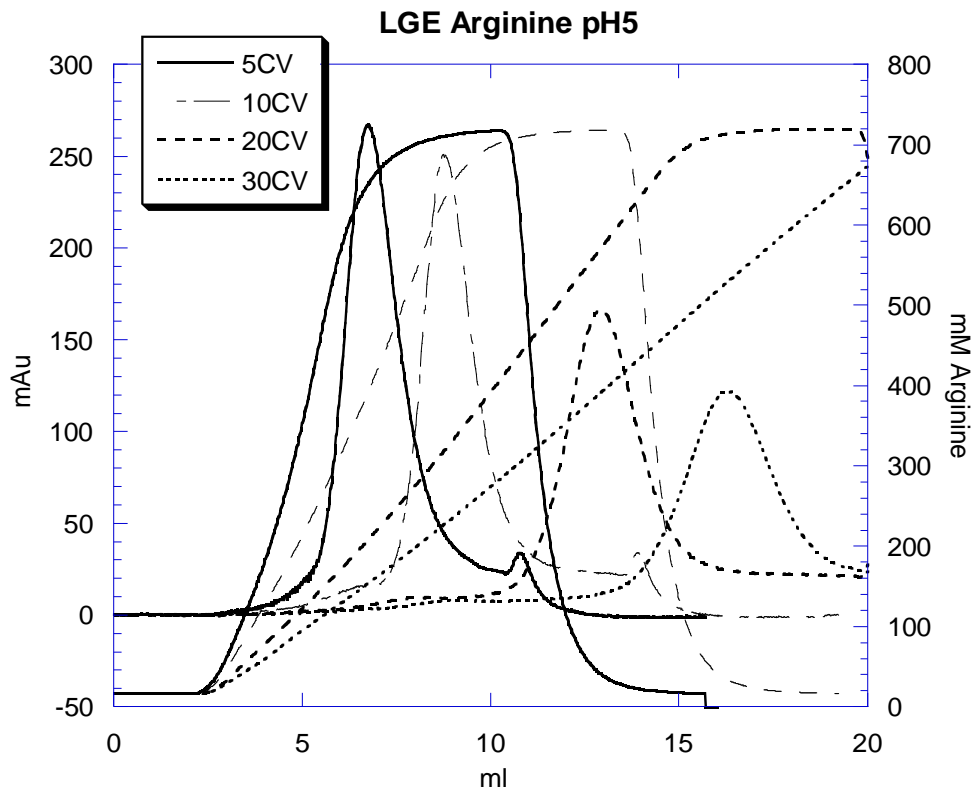


Figure 16: LGE chromatographic peaks for arginine

The salt concentration of each counterion at which the lysozyme elution peak is at its maximum was determined for every of the 4 gradient slopes. Furthermore the normalized gradient slope was calculated according to equation (8).

A log-log plot of the results (γ versus C_i) was made, in order to obtain the representative isotherms for LGE experiments, as can be seen in Figure 16. The data show conformity with the SMA model as this plot gives a straight line. This correlation is based on equation (9) which if solved logarithmically leads to a linear equation, where the slope is the charge of the protein.

A non-linear relationship should not be obtained in this case, as this would be a sign for errors in data evaluation or experimental performance.

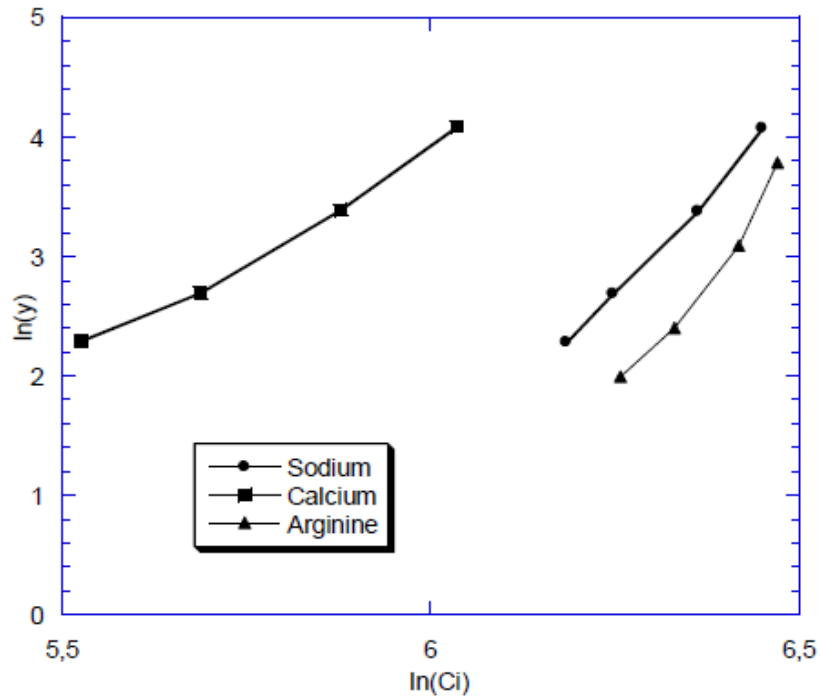


Figure 17: LGE summary normalized gradient slope vs. counterion concentration

According to the data analysis procedure described in chapter 5.3 the protein retention factor k' was calculated and plotted versus the concentration of each counterion, as summarized in Figure 17.

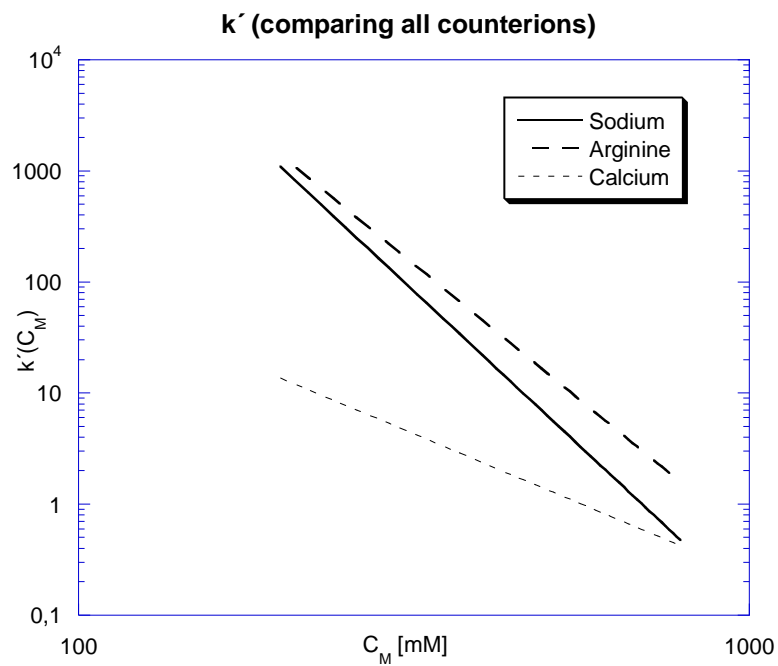


Figure 18: LGE summary retention factor vs. counterion concentration

Lines for sodium and arginine are very similar, in contrast to calcium which shows a lower slope. As the charge of sodium and arginine is likely the same, the slope which indicates the effective charge of the protein should also be the same. Due to the fact that k' is describing the state of a reaction (retention vs. elution) at equilibrium it is a dimensionless value.

The main results of the LGE experiments are summarized in Table 5 and 6.

Table 5: LGE summary retention factor as a function of the counterion concentration

C_M	$k' (C_M)$
20mM Sodium acetate pH 5	4.85E+08
20mM Arginine pH 5	1.20E+08
10mM Calcium acetate pH 5	2.67E+04
20mM Calcium acetate pH 5	4.64E+03

Lysozyme shows under 20mM sodium acetate pH 5 and 20mM arginine pH 5 the highest retention on Capto S, whereas at 20mM and 10mM calcium acetate it is more weakly bound. Comparing the two different concentrations for calcium, a tendency could be assumed, which shows that at lower ionic concentration of calcium, lysozyme is stronger bounded.

Table 6: LGE summary protein charge & equilibrium parameter

	z	A
Sodium acetate pH5	5.64	1.04E+16
Arginine pH5	4.94	3.24E+14
Calcium acetate pH5	2.53	8.96E+06

As shown in Table 6, the charge of lysozyme, obtained from the results for sodium and arginine, is around two times higher than for calcium. This can be explained as follows: One of the key assumption of the SMA model is that protein binding involves z-ligands in the exchange with the counterion. If we look at this reaction at the point of equilibrium, stoichiometric balance is given. Therefore the amount of z-ligands, counterions and the effective charge (represents the amino acids residues which interact with the stationary phase) of the protein is required to be at an equal level. Calcium, due to its bivalent charge involves two times more z-ligands at the stationary, compared to sodium. Therefore the protein has to “split” its charge, in order to maintain stoichiometric balance in the counterion exchange.

This leads to the results in Table 6, where lysozyme is half charged under calcium acetate pH 5. In the case of arginine and sodium pH 5, lysozyme shows similar charge, which is expected due to the fact that both counterions are monovalent.

The equilibrium parameter A is equal to the values for k' - higher for sodium and arginine, lower for calcium, which shows again that under calcium the protein is more weakly bound.

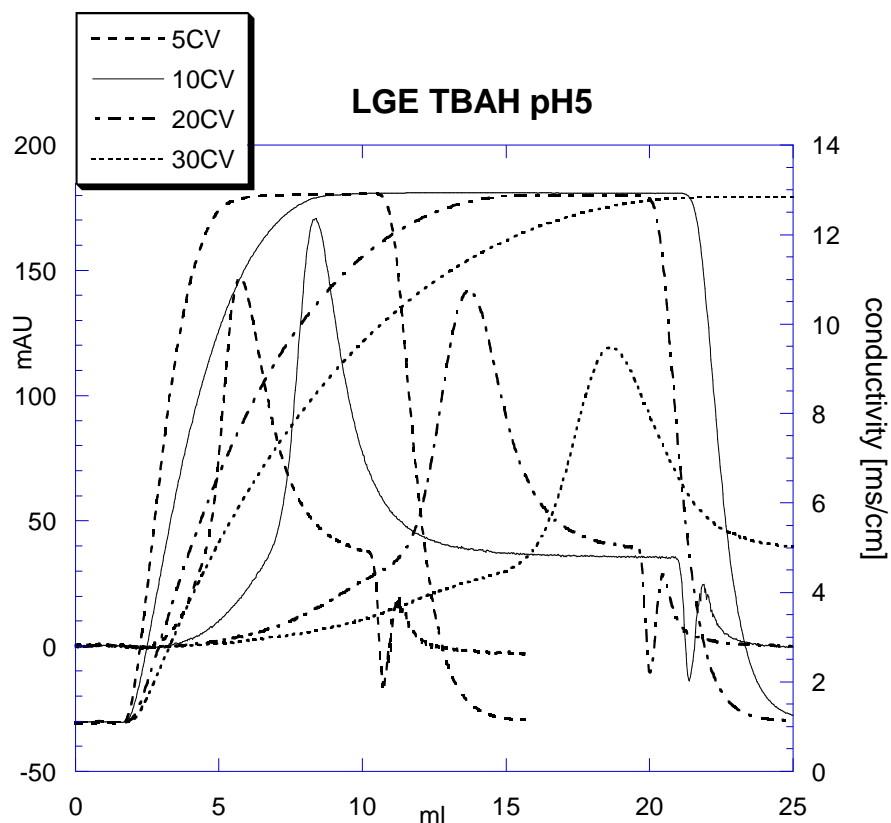


Figure 19: LGE chromatographic peaks for TBAH

5.3. Batch uptakes

Batch uptake curves were recorded on UNOsphere S and Captos S in 20mM Sodium acetate pH 5, 20mM Arginine pH 5, 20/10mM calcium acetate pH 5 and 20mM TBAH pH 5 according to the experimental description as mentioned in chapter 4.4. To describe the mass transfer rates an analytical solution is used, which is based on combining differential material balances for the protein in the adsorbent particles with an overall balance for the protein in the liquid phase. For the analysis of these experiments the rate equations (according to table 6.5 in ref. [3]) for film resistance and pore diffusion (solid curves) was coupled, taking into consideration the average particle size. Following curves were obtained (see figure 18&19). Capacities and Diffusivities are summarized in table 7&8.

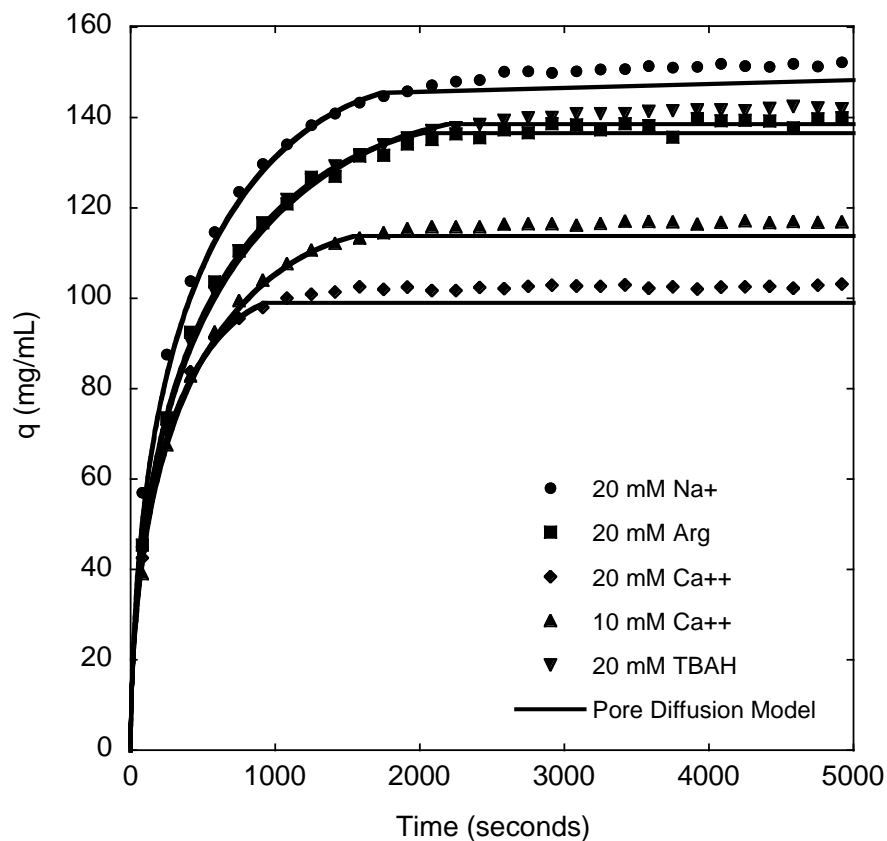


Figure 20: Batch uptake curves on UNOsphere S

Table 7: Summary of batch uptake results for UNOsphere S

UNOsphere S			
Counterion	q [mg/ml]	D_e [cm^2/s]	D_e / D_0
20mM Na^+	147	2.75E-07	0.24
20mM Arginine	138	2.25E-07	0.20
20mM Ca^{2+}	100	2.90E-07	0.25
10mM Ca^{2+}	115	2.30E-07	0.20
20mM TBAH	140	2.15E-07	0.19

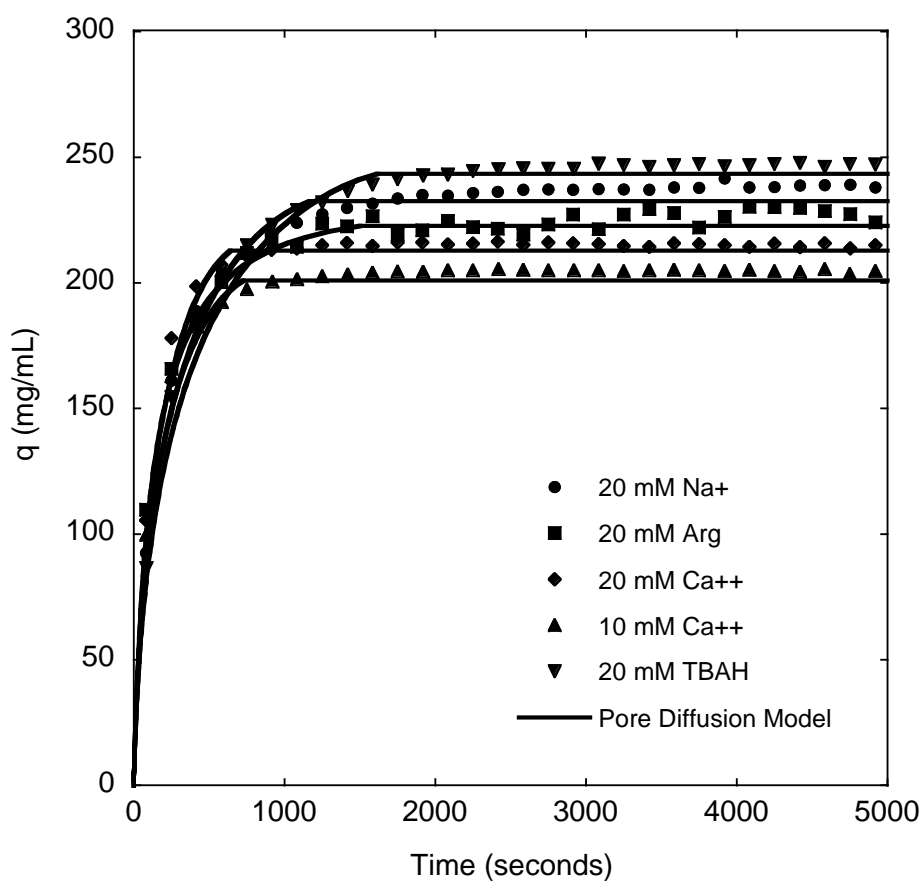


Figure 21: Batch uptake curves on Capto S

Sodium acetate shows the highest binding capacity, in contrast to calcium which shows the lowest ones. All capacities are comparable to results achieved at equilibrium obtained from isotherms. Due to the fact that all effective diffusivities are in the range between 2.15 to $2.90 \times 10^{-7} \text{cm}^2/\text{s}$, no immense influence by varying the type of the counterion could be measured. The fact that in all cases D_e/D_0 is smaller than 1 indicates that the diffusion inside the pores is severally hindered.

Table 8: Summary of batch uptake results for Capto S

Capto S			
Counter-ion	q [mg/ml]	D_e [cm^2/s]	D_e / D_0
20mM Na^+	258	7,00E-07	6,14E-01
20mM Arginine	233	1,50E-06	1,32E+00
20mM Ca^{2+}	230	1,50E-06	1,32E+00
10mM Ca^{2+}	220	1,20E-06	1,05E+00
20mM TBAH	266	7,00E-07	6,14E-01

In contrast to UNOsphere S, diffusion occurs faster in Capto S as can be seen in table 8. These results matches with the underlying key concept of solid diffusion, where the concentration gradient of the adsorbed protein gives such a large force that mass transfer occurs faster than in pore diffusion. For both cation exchangers the binding under calcium is weaker than under other counterions, the binding capacity increases as the calcium concentration goes down.

Compared to UNOsphere S the binding capacity in Capto S is higher due to dextran grafts, which provide a higher adsorptive surface.

All results for Capto S show $D_e/D_0 > 1$ which indicates that pore diffusion is not the determining diffusion mechanism in Capto S.

Calcium shows 1.3 to 1.5 larger diffusivities than for sodium, in the case of arginine D_e/D_0 is two times larger than for sodium, whereas TBAH shows the lowest diffusivity.

The amount of resin used for the batch uptake with arginine was calculated based on a lower estimation of the binding capacity for Capto S than actually given. Therefore the ratio V/V_M (see equation 12) was higher than the recommended change of 50% from initial to final protein concentration. This could have increased the experimental error and therefore leading to a non-conformity in the effective diffusivity for lysozyme under 20mM arginine pH 5 compared to the other results.

However, it can be concluded, that all diffusivities of each counterion are likely the same within the experimental error, although this cannot be verified as long as experiments are not repeated.

5.4. Summarized conclusions and outlook

The adsorption isotherms showed significant effects of the type of counterion on the adsorption of lysozyme for both UNOsphere S and Capto S. Similar binding capacities were seen for all three monovalent counterions (sodium, arginine and TBAH). However, a lower lysozyme binding capacity was seen for calcium when compared with the results for sodium at the same equivalent concentration of 20 mM (i.e. 20 mM Na⁺ and 10 mM Ca⁺⁺). The lower lysozyme capacity observed with calcium is attributed to the double charge of this ion. Accordingly, calcium is held more tightly by the resin making the protein-calcium-exchange less favorable than the protein-sodium-exchange. Increasing the calcium concentration to 20 mM further depressed the lysozyme binding capacity. This effect was attributed to the mass action law effect. Accordingly less lysozyme is bound at higher calcium concentrations.

This behavior was also evident from the LGE results which showed a lower effective lysozyme binding charge in the case of calcium than for either sodium or arginine. The monovalent counterions resulted in a binding charge of about 5 while calcium showed a lysozyme binding charge of about 2.5. The fact that the binding charge is halved is consistent with the divalent nature of calcium indicating that lysozyme adsorption on both resins is the result of a stoichiometric exchange of positively charged species. The lysozyme retention factor was also lower when calcium was used as the counterion instead of sodium or arginine. The two monovalent counterions showed similar retention factors. Since the retention factor determined from LGE is proportional to the initial slope of the isotherm, the LGE results are consistent with lysozyme binding being weaker when using calcium as a counterion as compared to the monovalent counterions.

In regard to the mass transfer kinetics, the following conclusions can be drawn based on the data obtained in this thesis:

1. The effective diffusivity of lysozyme in UNOsphere S is much smaller than its free solution diffusivity and practically independent of the type and concentration of the counterion. This behavior is consistent with a pore diffusion mechanism. Accordingly, lysozyme diffuses in the relatively large pores of UNOsphere S without direct interaction with the charged SP ligands. In this case the counterion has no effect since the lysozyme concentration in the pore fluid is very low and the counterion is in large molar excess.
2. The effective diffusivity of lysozyme in Capto S is about equal to or larger than its free solution diffusivity. In general, the effective diffusivity in a porous matrix is expected to be much lower than the free solution diffusivity since the pore network is expected to hinder transport. However, effective diffusivities higher than the free diffusivities when transport is enhanced by a solid diffusion mechanism. Accordingly, the protein diffuses while interacting with the SP-ligands attached to the Capto S matrix.
3. Interestingly, only a relatively small effect of the counterion type was seen on the effective diffusivity of lysozyme in Capto S. An effect would have been seen if the mass transfer flux were enhanced by either electrostatic coupling of fluxes or by a hopping mechanism. For the electrostatic coupling, the Nernst-Planck model would have predicted lower effective protein diffusivities for the bulkier monovalent counterions and for the divalent calcium. The fact that no significant differences were seen suggests that the Nernst-Planck model is not appropriate for describing diffusion of lysozyme in Capto S. The proposed hopping mechanism is also not consistent with the results. For this mechanism the expectation would have been that smaller effective lysozyme diffusivities would have been seen with the counterions for which the protein binds more strongly (i.e. Na⁺ and Arg⁺). The fact that no substantial difference was seen when comparing sodium and arginine with calcium despite the large difference in lysozyme binding strength suggests that the protein transport mechanism is not directly related to the strength with which the protein is bound.
4. One possibility is that protein binding capacity rather than protein binding strength is more directly responsible for protein transport in Capto S. The lysozyme binding capacity was lower for calcium ($q_m \sim 200$ to 220 mg/ml) compared to the capacities observed for sodium and TBAH ($q_m \sim 240$ and 250 mg/ml, respectively) but the effective diffusivity was higher for calcium ($D_e/D_0 \sim 1.3$ to 1.5) than for sodium and

TBAH ($D_e/D_0 \sim 1.0$ and 0.75 , respectively). This would suggest that higher effective diffusivities are obtained when the binding capacity is lower. Since a lower binding capacity corresponds to lower saturation of the binding sites, this experimental trend appears consistent with a mechanism where diffusion is facilitated by the availability of empty binding sites. The arginine results, however, seem to contradict this trend. In this case the lysozyme binding capacity was 230 mg/ml but $D_e/D_0 \sim 2.6$. On the other hand, this result could be affected by experimental error as only one experimental measurement was made.

Due to the fact that the diffusion of the counterion in protein adsorption is generally still not well known, a more detailed investigation could lead to a better understanding in this relation. For further experimental work it is recommended to repeat batch uptake kinetics for arginine and LGE experiments for TBAH, using at least a final gradient concentration of 1000 mM TBAH. Confocal laser scanning microscopy (CLSM) could be an opportunity in microscopic mass transfer measurement, in order to measure intra-particle concentration profiles, which could provide more detailed results.

6. References

- [1] Weiss J., 2004, *Handbook of Ion Chromatography*, Third Edition, Volume 1, Wiley-VCH Verlag
- [2] Carta G., 2011, *Protein Chromatography Short Course - Engineering Fundamentals and Measurements for Process Development and Scale-up*, University of Virginia
- [3] Carta G., Jungbauer A., 2010, *Protein Chromatography – Process Development and Scale-up*, Wiley-VCH Verlag
- [4] Tao Y., 2011, *Adsorption Equilibrium and Kinetics of mAb Charge Variants on Process-Scale Cation Exchangers*, Dissertation in Chemical Engineering, University of Virginia
- [5] Bio-rad company website, UNOsphere S datasheet,
http://www3.bio-rad.com/cmc_upload/Literature/42839/BULLETIN_2678.pdf, 20110731
- [6] GE lifescience company website, Capto S datasheet,
[http://www.gelifesciences.com/aptrix/upp00919.nsf/Content/71BF01E7D5F572C0C1257628001D1B46/\\$file/11002576AE.pdf](http://www.gelifesciences.com/aptrix/upp00919.nsf/Content/71BF01E7D5F572C0C1257628001D1B46/$file/11002576AE.pdf), 20110731
- [7] Carta G., Ubiera a. R., Pabst T. M., 2005, *Protein Mass Transfer Kinetic in Ion Exchange Media: Measurements and Interpretation*, Chemical Engineering & Technology, 28, 1255-1264
- [8] IUPAC Compendium of Chemical Terminology, 1997 second edition
- [9] Xijun Hu, Duong D. Do, Qiming Yu, 1992, *Effects of supporting and buffer electrolytes (NaCl, CH₃COOH and NH₄OH) on the diffusion of BSA in porous media*, Chemical Engineering Science, 47, 151-164
- [10] Helfferich F., 1995, *Ion Exchange*, First Edition, Dover Publications
- [11] Lenhoff, A.M., 2008, *Multiscale Modeling of Protein Uptake Patterns in Chromatographic Particles*, Langmuir, 24, 5991-5995
- [12] Parmar A.S., Muschol, 2009, *Hydration and hydrodynamic interactions of lysozyme: effects of chaotropic versus kosmotropics ions*, Biophysical journal, Biophysical Society, 97, 590-8
- [13] WebElements: the periodic table on the web
http://www.webelements.com/calcium/atom_sizes.html, 20110614
- [14] Duong D. Do, 1998, *Adsorption Analysis: Equilibria and Kintetics*, Series on Chemical Engineering, Vol., Imperial College Press
http://www.spektrum.de/artikel/848853&_z=798888, 20110515
- [15] Lund E.W., 1965, *Guldberg and Waage and the law of mass action*, Journal of Chemical Education 42, no.10, 548, doi:10.1021/ed042p548

[16] Brooks C., Cramer S., 1992, *Steric mass-action in ion exchange: Displacement profiles and induced salt gradients*, AIChE Journal 38, no.12, 1969-1978